

**Mixedmode oscillations in an electrochemical system. I. A Farey sequence which does not occur on a torus**

F. N. Albahadily, John Ringland, and Mark Schell

Citation: *The Journal of Chemical Physics* **90**, 813 (1989); doi: 10.1063/1.456106

View online: <http://dx.doi.org/10.1063/1.456106>

View Table of Contents: <http://scitation.aip.org/content/aip/journal/jcp/90/2?ver=pdfcov>

Published by the AIP Publishing

---

**Articles you may be interested in**

[Mixed-mode oscillations and cluster patterns in an electrochemical relaxation oscillator under galvanostatic control](#)

*Chaos* **18**, 015103 (2008); 10.1063/1.2779856

[Period adding and broken Farey tree sequence of bifurcations for mixed-mode oscillations and chaos in the simplest three-variable nonlinear system](#)

*J. Chem. Phys.* **112**, 6122 (2000); 10.1063/1.481222

[Mixedmode oscillations in chemical systems](#)

*J. Chem. Phys.* **97**, 6191 (1992); 10.1063/1.463727

[The modeling of mixedmode and chaotic oscillations in electrochemical systems](#)

*J. Chem. Phys.* **96**, 7797 (1992); 10.1063/1.462377

[Mixedmode oscillations in an electrochemical system. II. A periodic–chaotic sequence](#)

*J. Chem. Phys.* **90**, 822 (1989); 10.1063/1.456107

---



# Mixed-mode oscillations in an electrochemical system. I. A Farey sequence which does not occur on a torus

F. N. Albahadily, John Ringland, and Mark Schell

Department of Chemistry, Southern Methodist University, Dallas, Texas 75275

(Received 18 July 1988; accepted 30 September 1988)

We analyze measurements of an oscillatory current in an electrochemical process in which copper dissolves into phosphoric acid from a rotating-disk electrode. The focus is on a set of states in which each member consists of a different combination of large and small oscillations (mixed-mode oscillations). This set of mixed-mode oscillations is shown to constitute a Farey sequence, i.e., a periodic sequence for which a one-to-one correspondence exists with an ordered sequence of rational numbers. Plots of a measured quantity known as the "firing number" are presented which reveal a structure that is similar to a "devil's staircase." The states surrounding the mixed-mode oscillations are analyzed by examining one-dimensional maps, surfaces of section, and phase portraits constructed from experimental data. This analysis shows that the Farey sequence of these mixed-mode oscillations is of a different nature than the Farey sequences associated with phase locking on a torus.

## I. INTRODUCTION

In recent years considerable effort has been applied to categorizing and interpreting different types of complex dynamical behavior exhibited by dissipative systems held far from equilibrium. Several studies have focused on temporal behavior consisting of "large" and "small" oscillations with a substantial range of intermediate amplitudes unrealized.<sup>1-9</sup> We call this oscillatory behavior "mixed-mode oscillation." Mixed-mode oscillations (MMOs) have been observed in several experiments on isothermal chemical reactions,<sup>1,2,10-15</sup> most of which were carried out in continuously stirred, tank reactors. Sequences of different MMOs are observed while incrementing a constraint, such as the residence time of the reactor. Most sequences identified to date can be assigned to one of two classes: (1) "periodic-chaotic sequences," in which intervals of periodicity are separated by an interval of chaotic states which resemble random mixtures of the adjacent periodic patterns, and (2) "Farey sequences," which we define as periodic sequences for which a one-to-one correspondence with ordered sequences of rational numbers can be established.

Periodic-chaotic sequences were first observed in the Belousov-Zhabotinskii (BZ) reaction by Hudson *et al.*<sup>10</sup> More recent experiments on the same system by Swinney and Maselko<sup>1,2</sup> revealed a Farey sequence of MMOs. Farey sequences are familiar in periodically forced systems where periodic states are associated with "locking" of the driving frequency with an intrinsic frequency of the autonomous system. Here the phase-space trajectories of the combined system lie on a torus. Maselko and Swinney interpreted the behavior of their (undriven) chemical system in these terms except that the locking was between two intrinsic frequencies of the system itself. This interpretation was extended by Barkley<sup>9</sup> who offered an explanation of the apparent lack of quasiperiodic states in the Maselko-Swinney data.

In this paper, we describe observations of a Farey sequence in a completely different process involving hydro-

dynamics and electrochemistry: the anodic dissolution of copper from a rotating disk in phosphoric acid. As in the BZ reaction, the states of this Farey sequence have (to experimental resolution) full measure, i.e., there are no gaps where "nonsequence" states exist. In this case, however, the interpretation as phase locking on a torus is contraindicated by the nature of the surrounding states.

Oscillations in the current that accompany the dissolution of copper in phosphoric acid under an applied potential were observed quite some time ago,<sup>16</sup> and they are important in regard to practical applications as they occur close to the electropolishing region<sup>16-21</sup> (a range of values of the electrolyte concentration and the applied potential for which there is no etching of the copper surface, but instead, the surface becomes progressively smoother). One of the earliest theories of electropolishing of copper in phosphoric acid<sup>17</sup> postulates that a limit exists for the solubility of the major compound(s) formed by the dissolution process. It then follows that the current will increase with respect to increases in the potential set at the anode only to the extent that is allowed by the rate of transporting copper compounds from the thin boundary layer located at the surface of the anode to the bulk of the solution. At the limiting current the rate of dissolution will then be greater for portions of the surface that extend further into the solution. Specific details of the electropolishing theory (e.g., the species formed in the boundary layer) are still not known and furthermore, some researchers have disputed qualitative aspects of the theory.<sup>20</sup> Consequently, the electropolishing of copper and the related oscillatory phenomena remain current research topics.<sup>19,22-24</sup>

A variety of both regular and irregular temporal behaviors has been observed in a large number of electrochemical systems.<sup>25,26</sup> However, the more complicated oscillatory states have begun to be characterized only recently through the application of techniques from nonlinear dynamics.<sup>23,27-29</sup> In addition to using these techniques, we found that the identification of complex dynamical states in the copper-phosphoric acid system was further facilitated by

lowering the temperature. At room temperature it is difficult to determine whether the system is exhibiting "asymptotic behavior," long lasting transient behavior, or behavior that results from surface fluctuations (deformations of the surface of the copper electrode). One possible cause of these problems is the large amplitudes in the oscillations; a large amplitude entails the current passing through values whose maintenance would result in etching of the copper surface. Amplitudes are decreased by more than an order of magnitude at lower temperatures ( $< -17.0^\circ\text{C}$ ), and the behavior of the system is closer to an ideal limit in which the anode dissolves smoothly. At lower temperatures we were able to characterize a Hopf bifurcation, period-doubling bifurcations and chaotic states in the copper-phosphoric acid system.<sup>29</sup> Several waveforms of MMOs were also obtained. However, we did not investigate the detailed sequences of these MMOs nor the bifurcation structure local to these oscillations.

The purposes of the experimental investigation discussed in this paper were to examine in detail sequences of MMOs that occur in the copper-phosphoric acid system and to extract information on the structures in state space that support these oscillations, as well as to compare them with MMOs that have been observed in isothermal nonlinear chemical reactions.

Those aspects of the experimental setup and procedures that were different from those of Ref. 29 are described in Sec. II of this paper.

Several measured waveforms of MMOs are presented in Sec. III. This set of MMOs is seen to constitute a Farey sequence. We also show plots of a quantity known as the firing number which characterizes these states.

A phase diagram is presented in Sec. IV that shows the region of parameter space in which MMOs were found and regions in which quasiperiodic motion and chaotic oscillations were observed. Chaotic behaviors are identified through the analysis of one-dimensional maps constructed from experimental data. The analysis suggests that the basic structure in phase space that supports MMOs is formed in the region of chaotic oscillations and that a map with two extrema is the strongly contracting-limit representation of this structure. If the MMOs corresponded to phase locking on a torus, the underlying one-dimensional map would not possess extrema.

In Sec. V, we summarize those aspects of our experimental results which demonstrate that the Farey sequences of mixed-mode oscillations in the copper-phosphoric acid system are of a different nature than the Farey sequence associated with phase locking on a torus.<sup>30</sup> Although the mixed-mode states may be a continuation of phase locking zones, Farey sequences of the mixed-mode states could only be observed beyond the limit where the torus breaks up. A brief comparison between the Farey states reported in this paper and those observed in the BZ reaction is also given.

## II. EXPERIMENTAL

The system consisted of a rotating copper disk<sup>31</sup> (the working electrode), a platinum counter electrode, and a sat-

urated calomel reference electrode, all of which were appropriately positioned in an electrochemical cell that contained a solution of 85% phosphoric acid. In all experiments, a potentiostat (PAR 273) was used to set the potential at the copper-disk electrode with respect to the calomel electrode and to monitor the current. The electrochemical cell, equipment and all materials that were used as well as experimental procedures that were followed are the same as those described in Ref. 29 with the following exceptions: (1) the system was thermostated at  $-20.0^\circ\text{C}$ , and (2) the system was prepared by holding both the potential  $V$ , set at the working electrode, and the rotation rate of the working electrode at the values 430 mV and 3000 rpm, respectively, for 30 min.

Both the depth to which the rotating copper disk penetrated the solution and the distance between the rotating disk and the reference electrode affected the results of measurements. These effects did not change the qualitative nature of the results in that the number of behaviors and the measure in parameter space of any particular behavior remained essentially independent of the depth and distance; changing these two quantities caused a shift in parameter space. All measurements reported in this paper were made with the depth of the working electrode and the distance between it and the reference electrode set at 3 mm and 1.5 cm, respectively.

In order to study the bifurcation structures it was necessary to make small incremental changes in the potential set at the working electrode. The potential was measured independently of the potentiostat on several occasions with an HP 3478A voltmeter and was always found to remain constant within 0.01 mV.

## III. MIXED-MODE OSCILLATIONS THAT BELONG TO A FAREY SEQUENCE

In this section we describe a set of MMOs which can be put in one-to-one correspondence with an ordered set of rational numbers. The results of measuring a quantity known as the firing number are also given, and these are used to show the way in which the measure of the set of MMOs varies in parameter space.

### A. Measured waveforms of mixed-mode oscillations

Measured waveforms representing a number of mixed-mode states are shown in Figs. 1 and 2. In order to discuss and characterize them, it is convenient to introduce some notation which follows that of Ref. 2. The clear dichotomy between small and large oscillations enables one to characterize a periodic state by listing the lengths of unbroken stretches of large and small oscillations in one period. Thus, the list  $L_1, S_1, L_2, S_2$ , which we write for clarity in the form  $L_1^S L_2^S$ , denotes a state whose cycle consists of  $L_1$  large oscillations followed by  $S_1$  small oscillations, followed by  $L_2$  large, followed by  $S_2$  smalls. For example, the state shown in Fig. 1(b), consisting of stretches of four large oscillations interspersed by single small oscillations, is denoted by  $4^1$ .

The waveforms shown in Figs. 1(a)–2(e), which constitute an ordered set, were recorded at successively higher

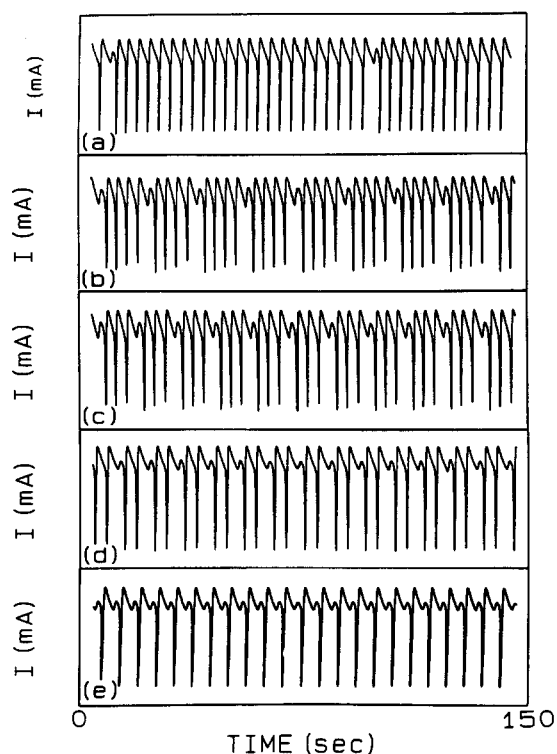


FIG. 1. Measured waveforms that correspond to a sequence of mixed-mode oscillations. Current  $I$  is plotted as a function of time. The current (ordinates) runs from  $-2.60$  to  $-0.55$  mA for all waveforms. Rotation rate = 1600 rpm. (a) A mixed-mode state that is close to the "limiting  $1^0$  state" (see the text for notation). The potential  $V$  set at the working electrode = 426.70 mV; (b) a  $4^1$  state,  $V = 427.00$  mV; (c) a  $3^1$  state,  $V = 427.05$  mV; (d) the  $2^1$  state,  $V = 427.25$  mV; (e) the  $1^1$  state,  $V = 428.75$  mV.

values of the working electrode potential  $V$ . All of these measurements were taken at the same value of the rotation rate (1600 rpm). As the potential was increased, the system passed through a sequence of states in which the ratio of large to small amplitude oscillations steadily decreased. Notice also that each state possesses a time series for which there is either only one small amplitude oscillation per set of large oscillations, as in Fig. 1, or only one large amplitude oscillation per set of small oscillations as in Fig. 2. All the MMOs observed in the copper-phosphoric acid system at the temperature  $-20.0^\circ\text{C}$  fall into one of these two categories.

## B. A Farey tree and firing numbers

In Fig. 3 we list the states observed as the potential was increased through the mixed-mode region. The list is laid out on a structure known as a Farey tree, which manifests the relationships that exist among the states. The working-electrode potential increases to the right in this figure (not to scale), while the vertical dimension is used solely for diagrammatic convenience. It is seen that the pattern of each state is the concatenation of the patterns of a pair of states above it, one on either side. Such a system of relationships was previously observed in the BZ reaction.<sup>2</sup> The waveforms of three states are shown in Fig. 4 each of which is a concatenation of two other states.

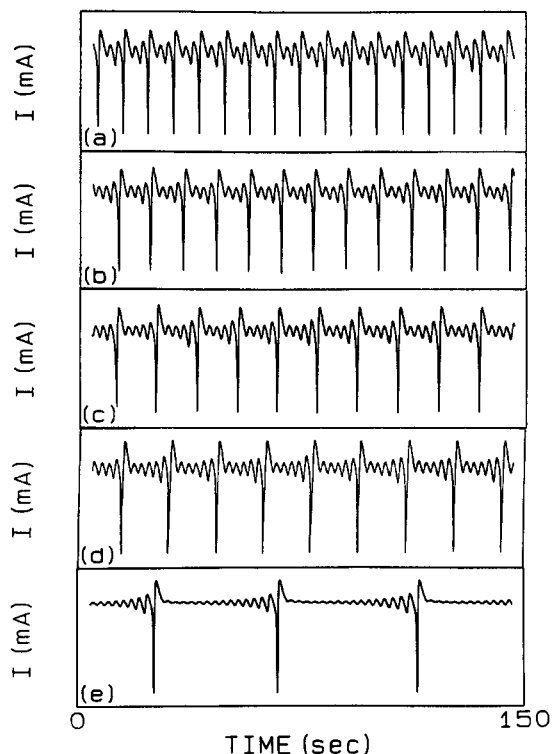


FIG. 2. A continuation of the sequence shown in Fig. 1. Rotation rate and the scale of the current are the same as Fig. 1. (a) A  $1^2$  state,  $V = 430.15$  mV; (b) a  $1^3$  state,  $V = 430.30$  mV; (c) a  $1^4$  state,  $V = 430.40$  mV; (d) a  $1^5$  state,  $V = 430.45$  mV; (e) a mixed-mode state near the end of the sequence,  $V = 430.49$  mV.

The Farey tree arises in number theory as an illustration of a scheme for the progressive generation of all the rational numbers between a given pair of rationals. This proceeds by the operation known as Farey addition<sup>32</sup>: the Farey sum of two rationals  $p/r$  and  $q/s$  is  $(p+q)/(r+s)$ ; the ratio of the numerators and denominators summed separately. The two starting rationals are written down at opposite sides of the page, then each stage of the process consists of writing between each pair of adjacent already-written numbers their Farey sum. A construction analogous to Fig. 3 follows if we

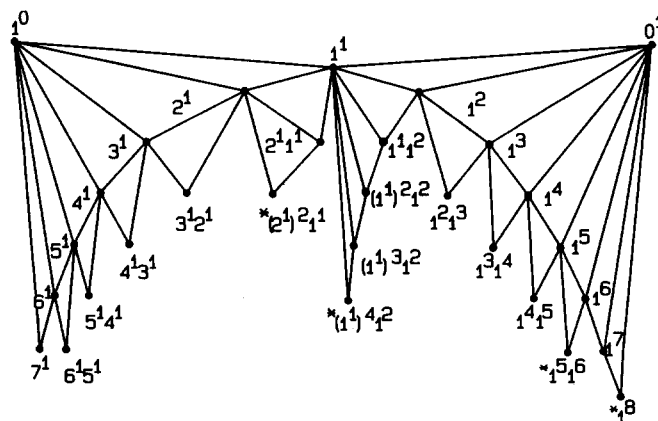


FIG. 3. A portion of the Farey tree constructed of observed states. States marked with a star were observed for only four to six cycles. Most other states were observed for many more cycles.

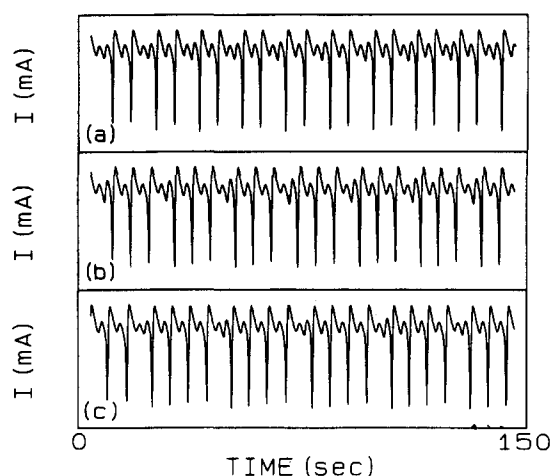


FIG. 4. Additional Farey states. Rotation speed and current scale are the same as Fig. 1. (a) the  $1^1 1^2$  state, which corresponds to the Farey sum of the  $1^1$  and  $1^2$  state,  $V = 429.70$  mV. (b) the  $1^1 1^1 1^2$  state, median of the  $1^1$  and  $1^1 1^2$  states,  $V = 429.57$  mV. (c) the  $1^1 1^1 1^1 1^2$  state,  $V = 429.47$  mV.

spread the numbers out in the vertical dimension and draw a line segment from each number to both of its "parents."

A correspondence between the mixed-mode states and the rational numbers may be established in the following way<sup>2</sup>: If one period of a state consists of a total of  $L$  large oscillations and  $S$  small oscillations, then we assign to that state the rational number

$$F = S / (L + S), \quad (1)$$

i.e., the fraction of the small oscillations. Following Ref. 2, we call this the firing number of the state. Since both the number of small oscillations per period and the total number of oscillations per period are additive under concatenation of patterns, the firing number of the "Farey mediant" of two states on the diagram of Fig. 3 will be the Farey sum of the firing numbers of its parents. A plot of the firing number of observed states versus the working-electrode potential will show two things. First, if the states do actually constitute a Farey sequence (i.e., they have the relationships represented by the Farey tree) the firing number will change monotonically with the parameter. Secondly, the relative and total "measure" of the set of periodic states will be made visible.

Figure 5 consists of four plots of the firing number vs potential for different values of the rotation speed. The experiments were carried out by varying the potential in small increments, and allowing at least four minutes (this length of time is four times longer than the time required to relax to either the  $1^1$  or the  $1^2$  state within most of their respective parameter range) for any transients to decay before determining the character of the oscillations. States with firing number  $> 0.83$ , though observed for rotation speeds  $> 1600$  rpm (see Fig. 2), are not represented in the figure, since a longer time was required for the reliable determination of these firing numbers.

The experimental results reveal that for rotation rates between 1600 and 2900 rpm, the width in potential of the MMOs and of the firing number 0.5 remains fairly constant. For much of this range, most states were readily classified as

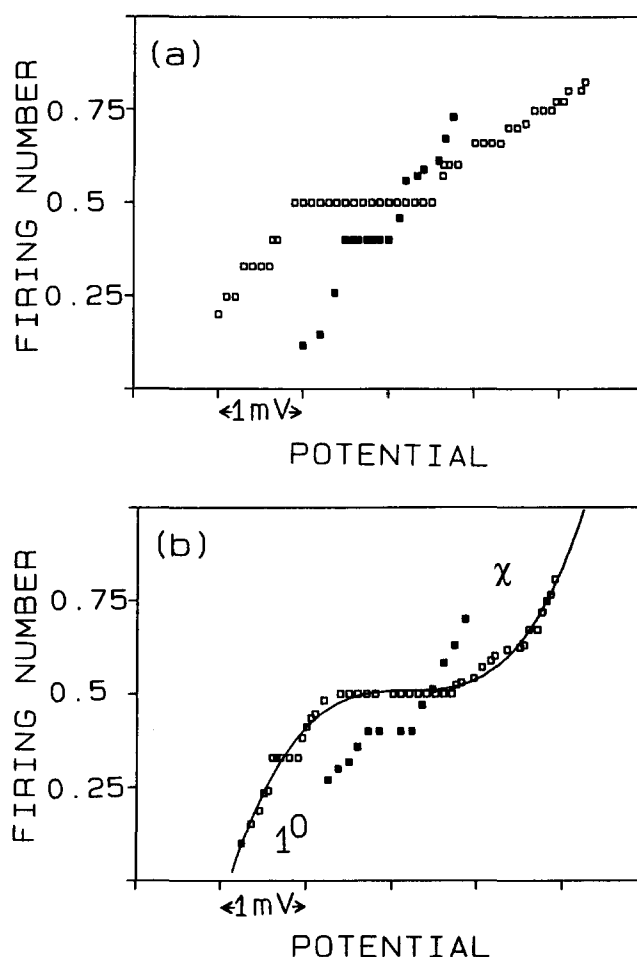


FIG. 5. Plots of the measured values of the firing number vs the potential set at the working electrode for four different values of the rotation rate. Note: We have plotted the closed rectangles below the actual value of the firing number by the amount 0.1 for clarity. (a) Open rectangles: rotation rate = 1900 rpm, potential range is from 437.0–443.0 mV. Closed rectangles: rotation rate = 3400 rpm; potential range is from 478.8–484.8 mV. (b) Open rectangles: rotation rate = 1600 rpm, potential range is from 425.5–431.5 mV. Closed rectangles: rotation rate = 1500 rpm; potential range is from 421.9–427.9 mV.  $\chi$  represents the fact that chaos was observed at the high firing end of the curve;  $1^0$  represents the fact that many small firing numbers observed in the other cases were not seen.

periodic members of a Farey sequence. However, even where this was true, the periodicity of some intermediate states was difficult to establish, though observations were not inconsistent with their being long-period members of the sequence, and no manifestly out-of-sequence states were observed. (We note that strictly speaking we are referring to periodicity of the pattern; a numerical analysis of the small oscillations in a set of MMOs found in a model of the BZ reaction showed that the amplitudes could vary chaotically, to a degree which might not be resolved experimentally.<sup>33</sup>)

Above 2900 rpm the sequence begins to become substantially squeezed, and for rates above 3400 rpm the sequence becomes too compressed to be analyzed reliably.

As the rotation rate was reduced from 1500 rpm, the highest observable firing number progressively decreased, until at 1300 rpm no MMOs were present. Adjoining the MMO region on the high firing number side, a region of

chaotic oscillations was seen which could be classified as mixed-mode states only in the vicinity of the boundary. Moving away from this boundary changed the behavior of the system in such a way that the dichotomy in the time series was lost, i.e., the division of a waveform into small and large amplitude oscillations was no longer possible. The chaotic states are discussed in more detail in Sec. IV. We also point out that we found that the  $1^1$  periodic region appeared to extend into the chaotic region, but the difference between the amplitudes decreased with the rotation rate, as did the width of the interval of potential values for which the state was found to exist.

The plots in Fig. 5 have a structure similar to that of the devil's staircase seen in models of phase locking.<sup>34</sup> In such models, gaps in the staircase consist of quasiperiodic states. We speculate, however, that if the resolution and stability of the experiment were to be further improved, gaps made visible in our staircases would correspond to chaotic states, rather than to quasiperiodicity. This is discussed in more detail in the next section.

#### IV. DYNAMICAL BEHAVIOR IN THE REGION OF THE PARAMETER SPACE CLOSE TO THAT OF THE FAREY STATES

In this section, we analyze measurements of dynamical behaviors observed for values of the constraints that surround those values for which mixed-mode oscillations occurred. The objectives are to find behaviors from which the mixed-mode oscillations evolve and to examine aspects of the structures in phase space that support them. The results show that in parameter space a region of chaotic oscillations separates the region of MMOs from a region of quasiperiodic oscillations. Only small distances separate the regions of MMOs and quasiperiodicity at higher rotation rates, and for some rotation rates it was difficult to determine whether an intermediate chaotic region even existed. Nevertheless, even for these cases, the evidence indicates that no stable torus was present in the region of MMOs. These results lead to the conclusion that the Farey states we observed are not of the same essence as those that arise due to phase locking on a torus.

##### A. Phase diagram

In Fig. 6, the parameter plane (rotation speed vs the potential  $V$  set at the working electrode) is divided into regions where distinct asymptotic behaviors were found. The mixed-mode oscillations as well as chaotic and quasiperiodic oscillations occurred within the thin, banana-shaped region. The way in which the regions of the three different types of behavior are arranged within the banana is revealed in the two insets of Fig. 6. While we have represented the quasiperiodic-chaotic and chaotic-MMO boundaries as smooth curves, we intend these curves only to indicate trends; the true boundaries can be quite convoluted on a small scale.

##### B. From steady-state to quasiperiodic behavior: Two Hopf bifurcations

Two sequential Hopf bifurcations occurred when the system was moved along a path from steady-state conditions

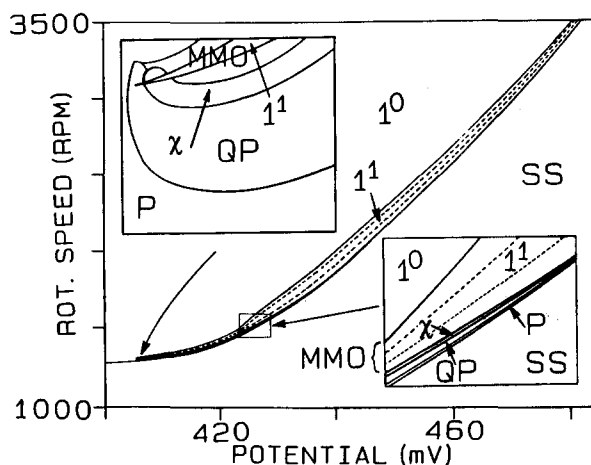


FIG. 6. The parameter plane (rotation speed vs the potential of the working electrode) divided into regions where different dynamical behavior was observed. The largest variety of behavior was found in the thin banana-shaped region, whose various parts are labeled in the lower right inset which is an enlargement of the rectangle indicated by the arrow. Parameter ranges in this rectangle: 424.0–429.5 mV, 1450–1600 rpm. P = periodic oscillations with small amplitudes. QP = quasiperiodic oscillations.  $\chi$  = chaotic oscillations. MMO = mixed-mode oscillations.  $1^1$  = a periodic mixed-mode state with 1 large amplitude oscillation and 1 small amplitude oscillation per cycle.  $1^0$  = a periodic state with one large amplitude oscillation per cycle. Note that at lower potentials we observed "P" to deform smoothly into " $1^0$ " as the rotation rate was increased. SS = stationary-state behavior. The inset in the upper left corner is an enlargement of the lower tip of the banana. Parameter ranges for this enlargement: 405.5–408.0 mV, 1280–1310 rpm.

towards the conditions associated with mixed-mode oscillations. The first Hopf bifurcation corresponded to the transition from steady-state behavior to sustained, small amplitude, nearly harmonic oscillations. Details of this bifurcation in the copper-phosphoric acid system are presented in Ref. 29.

The second Hopf bifurcation corresponded to a transition from periodic oscillations to quasiperiodic behavior. (The radius of the "limit cycle" in the "Poincaré section" was observed to increase from zero as the system was moved into the quasiperiodic region. No quantitative tests were performed to ensure that it was a Hopf bifurcation.) Two time series recorded beyond the bifurcation point are shown in

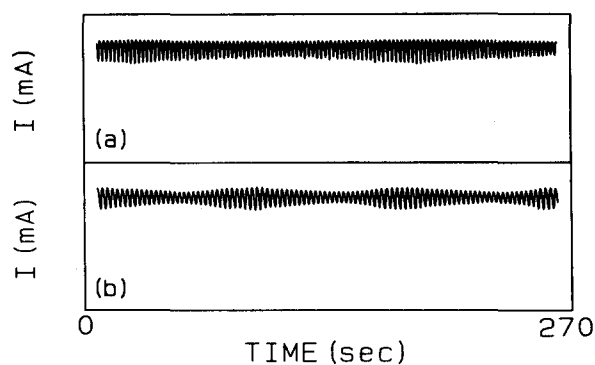


FIG. 7. Two quasiperiodic time series. (a) Rotation speed = 1360 rpm,  $V = 414.10$  mV. (b) Rotation speed 1500 rpm,  $V = 426.05$  mV.

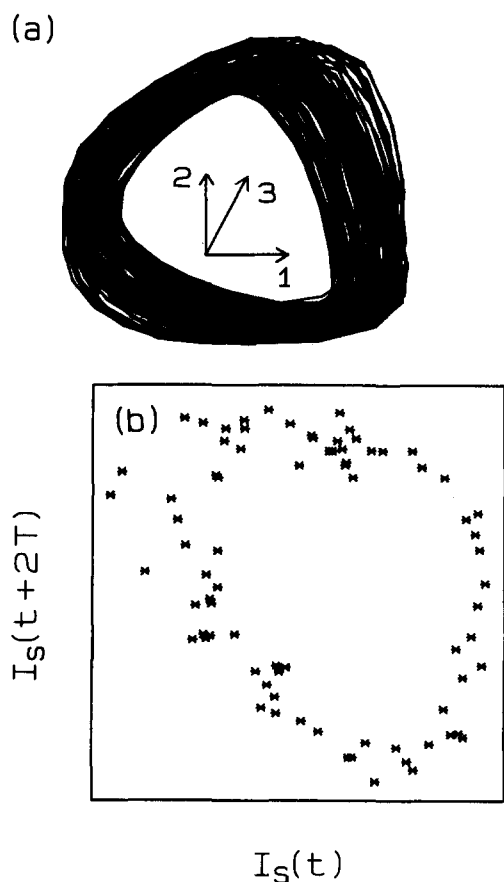


FIG. 8. Projection of a phase portrait of the state shown in Fig. 7(a). The time delay method was employed. Labels on the axes are defined as  $1 = I(t)$ ,  $2 = I(t + \tau)$ ,  $3 = I(t + 3\tau)$ .  $\tau = 13.8$  s. (b) Poincaré section constructed from the portrait in (a), at the surface defined by  $I(t + \tau) = -0.72$  mA.

Fig. 7. A phase portrait constructed using the time-delay method is shown in Fig. 8(a), and Fig. 8(b) shows the intersections of the trajectory thus generated with a surface of section. This Poincaré section is consistent with the existence of an attracting invariant torus.

### C. Chaotic states and initial formation of the structure that supports mixed-mode oscillations

A region, labeled  $\chi$ , exists in the parameter plane of Fig. 6 between the region of MMOs and quasiperiodic oscillations. We now analyze that part of this region shown in the upper left inset of Fig. 6. A measured time series is shown in Fig. 9(a). Notice that although the amplitudes are smaller than those of the periodic MMOs of Figs. 1 and 2, some segments of the time series can be divided into small and large amplitude oscillations. However, several oscillations have intermediate amplitudes. As the system was moved closer to the region labeled MMO in Fig. 6, the number of intermediate peaks in the time series became less numerous.

The analyses of one-dimensional maps constructed from the data support the interpretation that the behavior observed between the quasiperiodic region and the region of mixed-mode oscillations was chaotic oscillations. The map constructed by plotting the  $(n + 1)$ th minimum against the

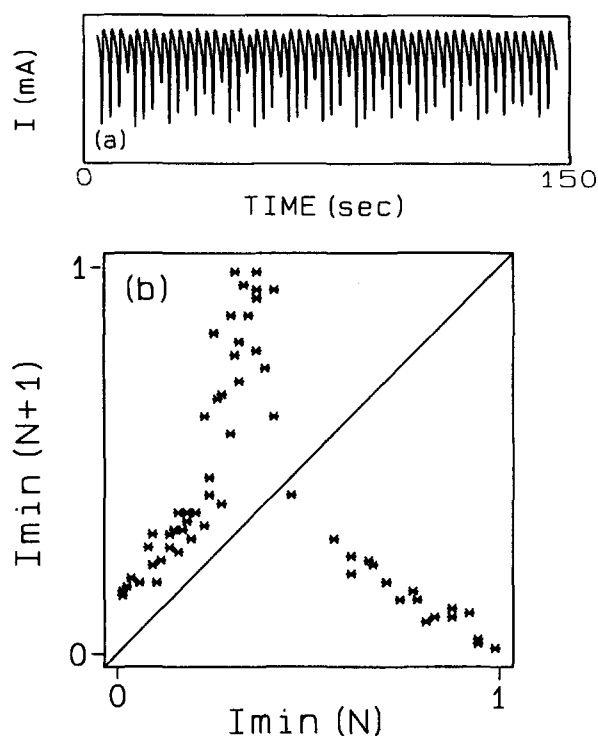


FIG. 9. (a) A time series from the chaotic region ( $\chi$ ) located in the upper left inset of Fig. 6. Current, which is on the same scale as Fig. 1, is plotted against time. Rotation rate = 1305 rpm;  $V = 405.84$  mV. (b) A one-dimensional map constructed from the time series in (a); the  $(n + 1)$ th minimum in the time series is plotted against the  $n$ th minimum.

$n$ th minimum of the time series of Fig. 9(a) is shown in Fig. 9(b). The iterates of the map delineate a map function that performs the stretching and folding which are the essentials of chaotic behavior.

In Fig. 10, we show three one-dimensional maps constructed from time series which were recorded at values of the constraints closer to the MMO region. The map in Fig. 10(a) was constructed from experimental data collected at a point in the tip of the  $\chi$  band above the incursion of the  $1^1$  region. The map in Fig. 10(b) is for a point in the  $\chi$  band on the other side of the  $1^1$  incursion, while Fig. 10(c) was constructed from data obtained at a point very close to the  $1^1$  incursion.

In order to see a connection between the properties of these maps and the properties of the mixed-mode oscillations, first consider iteration of the map in Fig. 10(a). An itinerary is generated in which two consecutive iterates can lie to the left of the midpoint of the interval whereas no two consecutive iterates can lie on the right side of the midpoint. If we then identify iterates to the left of the midpoint with large amplitude oscillations and those to the right with small amplitude oscillations, we reproduce the characteristic of the waveforms in Figs. 1(a)–1(e) of sequences of consecutive large amplitude oscillations separated by one small-amplitude oscillation. By construction, iterates of the map are the minima of oscillations and we point out that the consecutive iterates that land on the left of the midpoint increase in value, reflecting the increasing values of consecutive minima

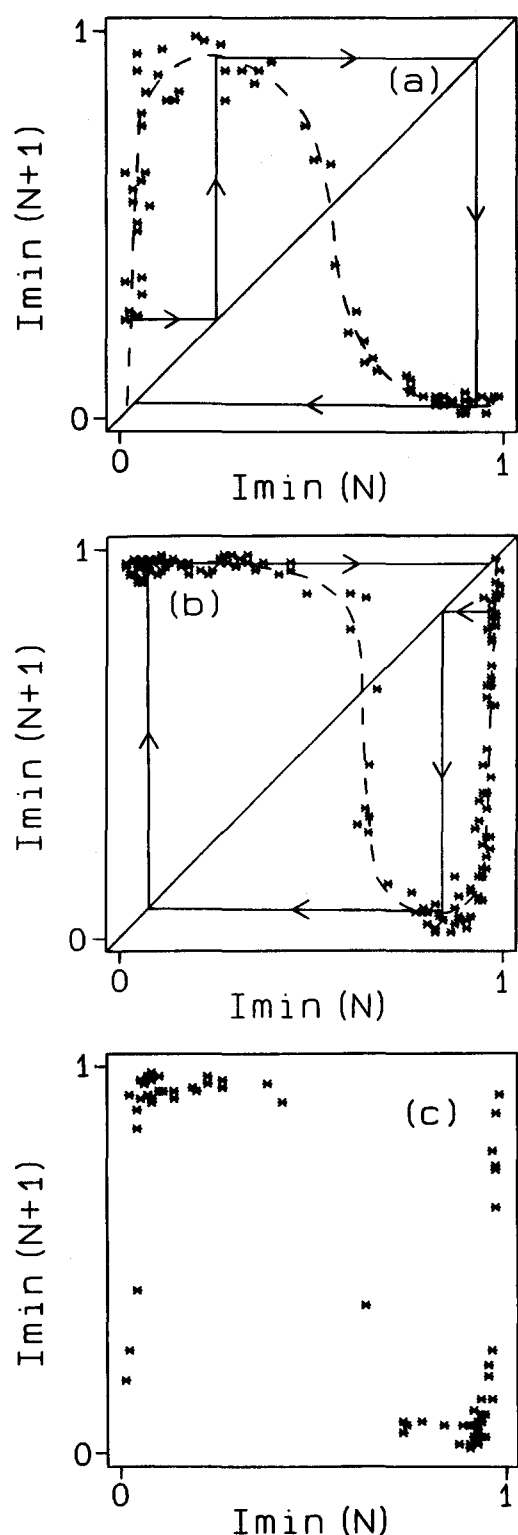


FIG. 10. Three one-dimensional maps constructed in the same way as in Fig. 9(b). (a)  $V = 405.93$  mV. Rotation speed = 1305 rpm. (b)  $V = 406.10$  mV. Rotation speed = 1303 rpm. (c)  $V = 406.00$  mV. Rotation speed = 1304 rpm.

which occurs in the consecutive large amplitude oscillations of Fig. 1.

A similar correspondence can be established between the itinerary of Fig. 10(b) and the mixed-mode oscillations shown in Fig. 2. The itinerary consists primarily of sequences

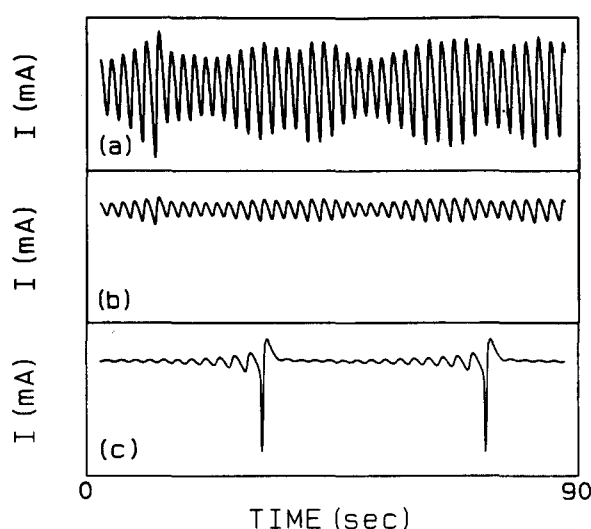


FIG. 11. "Quasiperiodic to MMO transition" at high rotation rate. (a) and (b) Time series just outside MMO region at 1600 rpm,  $V = 430.56$  mV, showing torus breaking up. (a) is a magnification of (b) which has the same current scale as used in Fig. 1. (c) Time series recorded at the same rotation rate with  $V = 430.49$  mV, showing nearly homoclinic MMO. Current scale the same as Fig. 1.

of consecutive iterates with decreasing value on the right side of the midpoint, separated by an iterate that lands on the left side of the midpoint. These properties correspond to those of Fig. 2 in which sequences of consecutive small amplitude oscillations, with decreasing values for their minima, are separated by solitary large amplitude oscillations.

Iteration of the map in Fig. 10(c) leads to an itinerary in which most consecutive iterates of the map alternate between the two sides of the midpoint; a state that is mostly  $1^1$ -like. This map appears to be a composite of the maps in Figs. 10(a) and 10(b). It is a map with two extrema, and such maps are known to be capable of supporting more than one asymptotic solution. However, an extensive search did not reveal bistability.

We were unable to determine the bifurcation mechanisms associated with the change from chaotic to periodic behavior. Clusters of points in the one-dimensional map, such as the two clusters near the extrema in Fig. 10(c), were observed to gradually shrink to single points as the periodic region was approached. Nevertheless, the results indicate that the maps of Fig. 10 prefigure one-dimensional maps underlying the MMOs. (We found that the dichotomy of amplitudes was too great in the MMO region to obtain meaningful maps there. Since the states were predominantly periodic, we subjected the system to perturbations in an attempt to sample underlying maps; a technique used, e.g., in Ref. 35.) It appears that the steepness of the middle segment of the map's domain underlies the formation of the dichotomy of amplitudes observed in the MMO region. The closer the middle branch becomes to being vertical the less the probability becomes for an iterate to land on this part of the map function. This steepness in the middle branch increased as the system was moved closer to the region of periodic MMOs.



### D. High rotation rates

The interposition of chaos between quasiperiodicity and MMO is evidence against the interpretation of the MMOs as phase locking on the torus. However, at high rotation rates the width (range in potential) of the chaotic band (as well as that of the quasiperiodic band) becomes smaller, eventually to the point where no chaotic interval of the kind represented by Figs. 10 is evident, and in this sense the quasiperiodic region borders directly on the MMO region.

Nevertheless even here, as evidenced by Figs. 11, the transition from quasiperiodicity to MMO is associated with the break up, loss of stability, and/or disappearance of the torus. The transition is very sharp and occurs with no observable hysteresis (i.e., no bistability). The figure shows two time series [Fig. 11(a) is a magnification of Fig. 11(b)] recorded in the vicinity of the transition at potentials differing by only a small fraction of a millivolt. The waveform in Figs. 11(a) and 11(b) shows the character of the irregularity that is seen just before the MMO region is entered, and demonstrates that a smooth attracting torus does not exist at this point. Furthermore, the waveform in Fig. 11(c) possesses characteristics that imply that a homoclinic orbit exists in the surrounding local region of parameter space which in turn is evidence that chaos exists in this local region (see Ref. 29). Many unresolved bifurcations may occur in the very thin transition region that exists between the value of the potential used in Fig. 11(b) and that used in Fig. 11(c) and a variety of scenarios is possible,<sup>36</sup> but our point here is that the dynamics changes to a major degree as the MMO region is entered. It does not simply correspond to entering a phase-locked tongue on the torus.

### V. SUMMARY OF THE ANALYSIS OF FAREY STATES AND A COMPARISON WITH MIXED-MODE OSCILLATIONS IN THE BELOUSOV-ZHABOTINSKII REACTION

We have described the observation of Farey sequences of mixed-mode oscillating states in the copper-phosphoric acid system. Plots of measured firing numbers were found to have a structure similar to that of the devil's staircase. Farey sequences and devil's staircases have been discovered in several theoretical investigations of the dynamics associated with attracting tori.<sup>37</sup> Models predict a complete staircase just prior to the breakup of the torus (see also Ref. 9). After the torus breaks up chaos is possible.<sup>38</sup> Before the breakup, phase-locked steps are separated by regions of quasiperiodicity. It is the merging of all phase-locked zones which results in the complete staircase.

Using only the results presented in Sec. III, it would seem reasonable to suggest the torus as the structure that supports the mixed-mode oscillations. However, the analyses in Sec. IV are not consistent with this suggestion since they demonstrate the Farey states were observed for ranges of parameter values that were well beyond those values for which the torus breaks up. Our experimental results also show that a map with two extrema is obtained in a limit as the representation of the structure that supports the MMOs. If the structure was a two-torus, the underlying one-dimensional map would not have extrema.

That the  $1^1$  state was found to extend into the quasiperiodic region (see Fig. 6) is consistent with the idea that the mixed-mode states may be continuations of phase locking zones in the quasiperiodic region. We were not able to determine whether other mixed modes states extended into the quasiperiodic region. Attempts were made to follow the extension of different mixed-mode states, but we would lose them in the chaotic region, where they formed extremely narrow bands. (We made no attempt to represent such incursions in Fig. 6.) No other phase-locked zones were found in the quasiperiodic region. However, even if the Farey states were present in this region, a nontrivial result of our study is the fact that the set of these states was observed to approach "full measure" well beyond the critical line at which the torus loses smoothness. The possibility of the existence of a Farey sequence within the supercritical region of a single phase-locked zone has recently been raised.<sup>39</sup>

States belonging to a Farey sequence with the qualitative features of the waveforms shown in Figs. 1, 2, and 4 have been observed in the Belousov-Zhabotinskii reaction.<sup>1,2</sup> States were also observed in that system in which *both* large and small oscillations occur consecutively. We have observed no such states in the copper-phosphoric acid system at low temperatures.

Elsewhere in the copper-phosphoric acid system, on the higher-rotation-rate shore of the  $1^0$  state (well beyond the range of Fig. 6), we have observed sequences of MMOs with alternating periodic and chaotic bands. These will be described in a future paper.

### ACKNOWLEDGMENTS

Acknowledgment is made to both The Robert A. Welch Foundation (Grant No. N-1096) and the Donors of The Petroleum Research Fund, administered by the American Chemical Society, for their support of this research.

<sup>1</sup>H. L. Swinney and J. Maselko, Phys. Rev. Lett. **55**, 2366 (1985); J. Maselko and H. L. Swinney, Phys. Scr. **52**, 269 (1984).

<sup>2</sup>J. Maselko and H. L. Swinney, J. Chem. Phys. **85**, 6430 (1986); Phys. Lett. A **119**, 403 (1987).

<sup>3</sup>R. J. Bagley, G. Mayer-Kress, and J. D. Farmer, Phys. Lett. A **114**, 419 (1986).

<sup>4</sup>R. Larter, C. L. Bush, T. R. Lonis, and B. D. Aguda, J. Chem. Phys. **87**, 5765 (1987).

<sup>5</sup>K. Bar-Eli and R. M. Noyes, J. Chem. Phys. **88**, 3646 (1988); R. D. Janz, D. J. Vanecek, and R. J. Field, *ibid.* **73**, 3132 (1980); J. Rinzel and W. C. Troy, *ibid.* **76**, 1775 (1982).

<sup>6</sup>K. Tomita and I. Tsuda, Prog. Theor. Phys. **64**, 1138 (1980).

<sup>7</sup>K. Showalter, R. M. Noyes, and K. Bar-Eli, J. Chem. Phys. **69**, 2514 (1978); V. Gaspar and K. Showalter, *ibid.* **88**, 778 (1988).

<sup>8</sup>P. DeKepper and K. Bar-Eli, J. Phys. Chem. **87**, 480 (1983).

<sup>9</sup>D. Barkley, Phys. Lett. A **129**, 219 (1988).

<sup>10</sup>P. DeKepper, A. Rossi, and A. Pacault, C. R. Acad. Sci. Paris C **282**, 199 (1976).

<sup>11</sup>J. L. Hudson, M. Hart, and D. Marinko, J. Chem. Phys. **71**, 1601 (1979); J. L. Hudson and J. C. Mankin, *ibid.* **74**, 6171 (1981).

<sup>12</sup>C. Vidal, J. C. Roux, A. Rossi, and S. Bachelart, C. R. Acad. Sci. Paris C **289**, 73 (1979); J. C. Roux, Physica D **7**, 57 (1983); C. Vidal, J. C. Roux, S. Bachelart, and A. Rossi, Ann. N. Y. Acad. Sci. **357**, 377 (1980); H. L. Swinney and J. C. Roux, in *Nonequilibrium Dynamics in Chemical Systems*, edited by C. Vidal and A. Pacault (Springer, New York, 1984), p.

- 124; F. Argoul, A. Arneodo, P. Richetti, J. C. Roux, and H. L. Swinney, *Acc. Chem. Res.* **20**, 436 (1987).
- <sup>13</sup>M. Orban and I. R. Epstein, *J. Phys. Chem.* **86**, 3907 (1982); M. Almgir and I. R. Epstein, *J. Am. Chem. Soc.* **105**, 2500 (1983); I. R. Epstein in *Nonequilibrium Dynamics in Chemical Systems*, edited by C. Vidal and A. Pacault (Springer, New York, 1984), p. 24.
- <sup>14</sup>H. L. Swinney, *Physica D* **7**, 3 (1983).
- <sup>15</sup>H. Degn, L. F. Olsen, and J. W. Perram, *N. Y. Acad. Sci.* **316**, 623 (1979); L. F. Olsen, *Phys. Lett. A* **94**, 454 (1983).
- <sup>16</sup>P. Jacquet, *Bull. Soc. Chim. Fr.* **3**, 705 (1936).
- <sup>17</sup>W. C. Elmore, *J. Appl. Phys.* **10**, 724 (1939); **11**, 797 (1940).
- <sup>18</sup>E. C. Williams and M. A. Barrett, *J. Electrochem. Soc.* **103**, 363 (1956).
- <sup>19</sup>S. H. Glarum and J. H. Marshall, *J. Electrochem. Soc.* **131**, 691 (1984); **132**, 2872, 2878 (1985).
- <sup>20</sup>J. Edwards, *J. Electrochem. Soc.* **100**, 223C (1953); C. Wagner, *ibid.* **101**, 225 (1954).
- <sup>21</sup>P. Poncet, M. Braizaz, B. Pointu, and J. Rousseau, *J. Chim. Phys.* **75**, 287 (1978).
- <sup>22</sup>K. Kojima and C. W. Tobias, *J. Electrochem. Soc.* **120**, 1026 (1973).
- <sup>23</sup>A. L. Kawcznski, M. Przasnyski, and B. Baranowski, *J. Electroanal. Chem.* **179**, 285 (1984).
- <sup>24</sup>L. T. Tsitsopoulos, T. T. Tsotsis, and T. A. Webster, *Surf. Sci.* **191**, 225 (1987).
- <sup>25</sup>C. G. Law and J. Newman, *J. Electrochem. Soc.* **126**, 2150 (1979); J. Wojtowicz and B. E. Conway, *J. Chem. Phys.* **52**, 1407 (1970); B. Conway and D. M. Novak, *J. Phys. Chem.* **81**, 1459 (1977); J. Wojtowicz, in *Modern Aspects of Electrochemistry*, edited by J. O'M. Bockris and B. Conway (Plenum, New York, 1973), Vol. 8, pp. 47-120; J. Keizer and D. Scherson, *J. Phys. Chem.* **84**, 2025 (1980).
- <sup>26</sup>P. Russell and J. Newman, *J. Electrochem. Soc.* **133**, 59 (1986); **134**, 1051 (1987); H. P. Lee, K. Nobe, and A. J. Pearlstein, *ibid.* **132**, 1031 (1985); J. B. Talbot, R. A. Oriani, and M. J. DiCarlo, *ibid.* **132**, 1545 (1985).
- <sup>27</sup>C. B. Diem and J. L. Hudson, *AI ChE. J.* **33**, 218 (1987); M. R. Bassett and J. L. Hudson, *Chem. Eng. Comm.* **60**, 145 (1987); (preprint, 1987); (preprint, 1988); J. L. Hudson, J. C. Bell, and N. I. Jaeger (Berichte der Bunsen-Gesellschaft, preprint, 1988).
- <sup>28</sup>M. Sheintuch and J. Schmidt, *J. Phys. Chem.* **92**, 3404 (1988); O. Lev, M. Sheintuch, L. M. Pismen, and A. Wolffberg (preprint, 1988).
- <sup>29</sup>F. N. Albahadily and M. Schell, *J. Chem. Phys.* **88**, 4312 (1988).
- <sup>30</sup>M. Dubois and P. Berge, *Phys. Lett. A* **76**, 53 (1980); H. Haucke and R. E. Ecke (preprint, 1987).
- <sup>31</sup>A. J. Bard and L. R. Faulkner, *Electrochemical Methods Fundamentals and Applications* (Wiley, New York, 1980), Sec. 8.3.
- <sup>32</sup>S. Kim and S. Ostlund (preprint, 1988).
- <sup>33</sup>P. Richetti, J. C. Roux, F. Argoul, and A. Arneodo, *J. Chem. Phys.* **86**, 3339 (1987).
- <sup>34</sup>P. Cvitanovic, M. H. Jensen, L. P. Kadanoff, and S. J. Shenker, *Physica D* **5**, 370 (1983).
- <sup>35</sup>I. B. Schwartz, *Phys. Lett. A* **102**, 25 (1984).
- <sup>36</sup>D. Barkley, J. Ringland, and J. S. Turner, *J. Chem. Phys.* **87**, 3812 (1987); V. Franceschini and C. Tebaldi, *Comm. Math. Phys.* **94**, 317 (1984); V. Franceschini, *Physica D* **6**, 285 (1983); W. Langford, in *International Series of Numerical Mathematics* (Birkhauser, Basel, 1984), Vol. 70.
- <sup>37</sup>M. H. Jensen, P. Bak, and T. Bohr, *Phys. Rev. A* **30**, 1960 (1984).
- <sup>38</sup>M. Schell, S. Fraser, and R. Kapral, *Phys. Rev. A* **28**, 373 (1988).
- <sup>39</sup>J. Ringland and M. Schell (preprint, 1988).